Original Article

Institution of MECHANICAL ENGINEERS
Journal of AEROSPACE ENGINEERING

Proc IMechE Part G:
J Aerospace Engineering
0(0) 1–17

DOI: 10.1177/0954410016662077
uk.sagepub.com/jaero
SAGE

Aerodynamic and stability analysis of personal vehicle in tandem-wing configuration

Tomasz Goetzendorf-Grabowski and Marcin Figat

Abstract

The paper presents a concept of tandem-wing configuration aircraft that was a Warsaw University of Technology proposal for the personal air transport system. The project was developed at Warsaw University of Technology, within the PPLANE project (FP7 – Personal Plane: Assessment and Validation of Pioneering Concepts for Personal Air Transport Systems). First, analysis of the general concept, advantages and disadvantages of tandem-wing configuration, and possible application as a personal air transport system vehicle are presented. Next, aerodynamic design is analyzed and dynamic stability is tested. All numerical analyses were made by use of the well-tested professional software for aerodynamic (MGAERO) and stability (SDSA) analyses.

Keywords

Aircraft design, personal air transport systems, tandem wing, stability, flying qualities, aerodynamics

Date received: 3 March 2016; accepted: 6 July 2016

Introduction

The personal air transport systems (PATSs) are going to be a new standard in the close future. Definition of the operational concept for the future PATS was one of the most important goals of the innovative PPLANE project.[1] The main idea of this project is to build a high level, fully autonomous system, which uses the quick air transport for passengers, goods, and others. The system has to consist of a dedicated network of PPorts and should include its own air traffic control system. All vehicles have to be fully automated and in the future fully autonomous. The ground pilots placed in remote pilot stations (RPSs) would only supervise the flight, but still be able to take over the control in nonstandard situations. The full description of PPlane project (assumptions, analysis, and conclusions) is available in official PPlane deliverables.[2,3]

Initial Considerations

One of the most important components of the PPlane system is the vehicle. It should meet the very high level of requirements. The choice of aircraft configuration has a huge influence on the whole system, especially on the infrastructure of PPlane ready airports (PPorts), etc. The requirements, which have been established within the PPLANE project[4], describe aircraft capacity, the number of engines, aircraft performance, environmental impact (e.g. CO_2 emission), manufacturing, and others. The survey conducted in the framework of PPLANE project showed that the customer needs related to vehicle are: safety, door-to-door time, wide range of destination, environment friendliness. Thus, reliable configuration, vertical take-off and landing (VTOL) characteristics, relatively high cruise airspeed, and electric propulsion were selected as the most important features of the new aircraft.

It is likely that one single PPlane configuration will not satisfy all the needs for an individual public air vehicle mainly due to cost effectiveness. It is anticipated that the PPlane fleet will be composed of 4 to 6 seat, mainly fixed wing aircraft. The rotary wing aircraft, VTOL vehicles will likely be reserved for special missions, which require high flexibility in the location of landing and take-off, such as for emergency medical evacuation or it may be also useful in the case of areas inside buildings or mountainous areas. A multi-engine fixed wing configuration has been chosen for two reasons. The main one is reliability and safety, as it would be difficult to guarantee a satisfactory safety level with a single engine configuration.

Faculty of Power and Aeronautical Engineering, Warsaw University of Technology, Warsaw, Poland

Corresponding author:
Tomasz Goetzendorf-Grabowski, Faculty of Power and Aeronautical Engineering, Warsaw University of Technology, Nowowiejska 24, 00-665 Warsaw, Poland.
Email: tgrab@meil.pw.edu.pl

The second reason is performance, as the propulsion can be distributed.

The design of the vehicle and selection of configuration was preceded by analysis and rating using house of quality process.[5] One of the candidates for PPlane vehicle was the multipurpose tilt rotor in tandem wing configuration proposed by Warsaw University of Technology (WUT)[6] (Figure 1).

The considered aircraft was designed as quad-tilt rotor, tandem wing configuration. The proposed configuration combines aircraft and helicopter capabilities. It can fly as a classic aircraft when at least two of the four rotors give forward thrust with relatively wide range of airspeeds, which can be achieved due to the high lift coefficient, obtained by tandem wing configuration. On other hand, it can fly like a helicopter when all rotors give vertical thrust. This concept allows the aircraft to have VTOL characteristics.

This unconventional configuration of the aircraft could be very useful for special purposes like police forces, fire brigades, air ambulance, etc. Figure 2 presents the conceptual visualization of the possible application.

Figure 1. Tilt rotor, tandem wing aircraft designed at WUT.

Introduction to tandem wing configuration

The concept of the Tandem wing configuration, presented above, is not a new idea. A very big enthusiast of tandem wing was British designer George Herbert Miles.[7] Few tandem wing aircrafts designed by Miles were built; however, they did not meet similar pilots' enthusiasm, due to the bad flying qualities and control problems. Until today, other aircraft designers have also designed and built similar aircrafts, but only a few of them have been completed with success. Numerous problems with stability caused, that the support of smart Automatic Flight Control System was necessary. Nowadays such systems are available. Good examples of tandem wing configuration aircrafts are Proteus[8] and Quickie. However, the most successful tandem wing configuration aircraft ever built is Rutan's Model 133 ATTT[9] (Figure 3). The idea was born in 1987, initiated and supported by DARPA project. It was assumed, that the

Figure 2. Conceptual view of air ambulance (on the left) and police force monitoring the traffic.

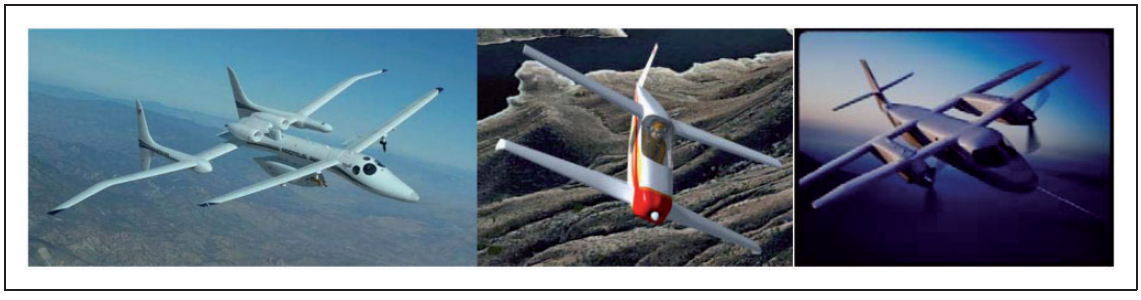

Figure 3. The most famous aircrafts in tandem-wing configuration (on the left Proteus, in the middle Quickie, on the right Model 133 ATTT (Courtesy of Scaled Composites, LLC.))

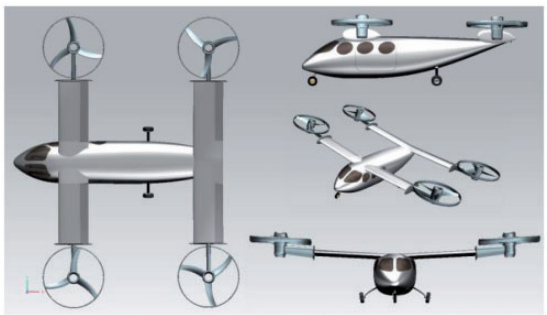

Figure 4. Tandem wing configuration and the basic geometric dimensions.

maximum take-off weight (MTOW) will be equal to 25 tons (including 5 tons of payload). The computed maximum L/D ratio was about 20 and maximum lift coefficient was equal to 3.55. Only a scaled technology demonstrator (0.62) was built. The project was very promising but it was cancelled due to unclear reasons.

Tandem wing configuration – the best choice for PPlane vehicle

One of the most promising vehicle for PPlane system was proposal developed at the Warsaw University of Technology. Its unconventional configuration, which combines advantages of tilt rotor and tandem wing configuration, should significantly increase the safety and performance of the whole PPlane system. Moreover, this configuration seemed to be more reliable than classic aircraft and may have a wider array of applications. The conceptual view is presented in Figure 4. The proposed configuration (tandem wing) allows the achievement of high maximum lift coefficient. The tilt rotor concept allows VTOL characteristics and performs the mission like a classic aircraft as well.

The maximum take-off weight of presented aircraft is about 1600 kg, while empty weight is equal to 1200 kg. It is designed in a four seat configuration with small payload. The total payload is assumed to be 400 kg (4 people + baggage/small payload). The aircraft is equipped with four electric motors located at the tips of each wing. The assumed maximum power of one motor is 150 kW, so the total maximum available power of designed aircraft is about 600 kW. All motors are powered by electrical energy stored in battery packs mounted inside the wings. To accomplish the assumed performance the total battery capacity should be approximately 2000 Ah (assumed voltage 180 V). This value of battery capacity is large; however, technology in this area is currently under very rapid development and taking into account, that the aircraft is designed for not so close future (about 20 years), the expectation of such capacity of batteries could be rational and reasonable.

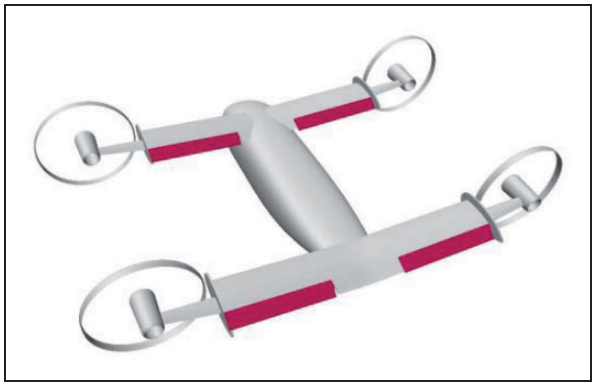

Figure 5. Aircraft control surfaces – two pairs of elevons.

Two methods of control have been taken into consideration. The first one, used particularly during the hover phase assumes the change of the thrust value or vector by rotation of the motors. This concept is not considered in this paper. The second method assumes the use of classic control surfaces. To control the aircraft, two pairs of elevons (Figure 5) on the front and rear wings have been considered. Both of them can be used to increase the lift coefficient and to trim or control in pitch channel (symmetrical case of deflection) as well. Lateral control (roll) may be achieved by asymmetrical deflection of all control surfaces.

Basic aircraft configurations

It was assumed, that the designed aircraft is able to accomplish the hover by both vertical take-off and by classic take-off from tarmac followed by transition to hover. The hover configuration means that all of the motor power and thrust of the rotors are used to give the lift. In this case, longitudinal, lateral stability, and trim are satisfied by differential thrust of all engines, sufficient stability augmentation, and control systems. This configuration will only be used for special cases because a lot of energy is needed to execute flight under such conditions. This flight configuration could be necessary during transport of injured people from a dangerous place to a landing field near a hospital. Figure 6 presents the phase transition from hover to horizontal flight.

Two basic configurations of horizontal flight are considered for WUT tilt rotor. Both are connected with aerodynamic features of the aircraft. The impact of all engines on the aerodynamic characteristics, stability and trim conditions were not considered at this stage.

The first configuration is called the low-speed configuration—LS. It will be used for low-speed flights for example to patrol the roads. During low-speed flight, only motors on the front wing are in use and rotors give thrust parallel to longitudinal axis.

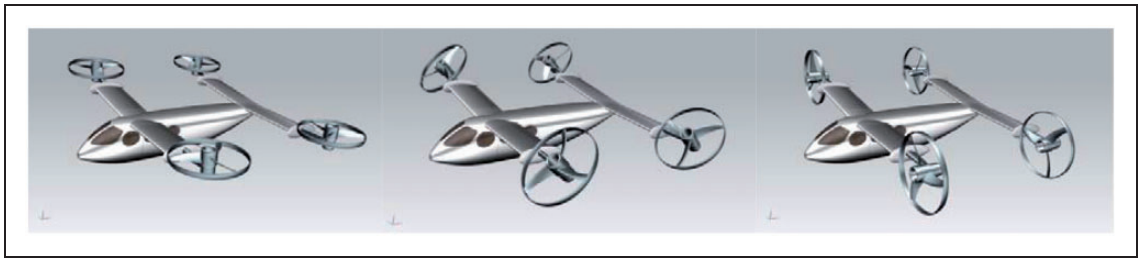

Figure 6. Transition from hover to horizontal flight.

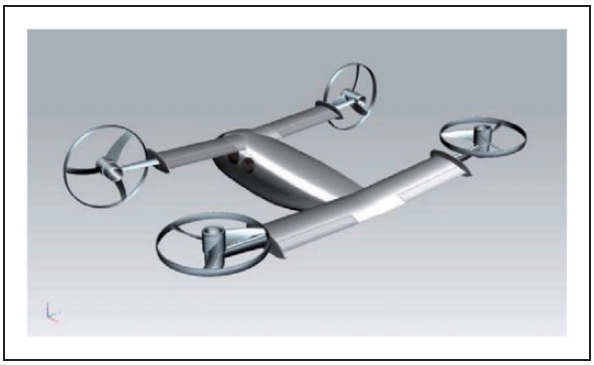

Figure 7. Low-speed configuration.

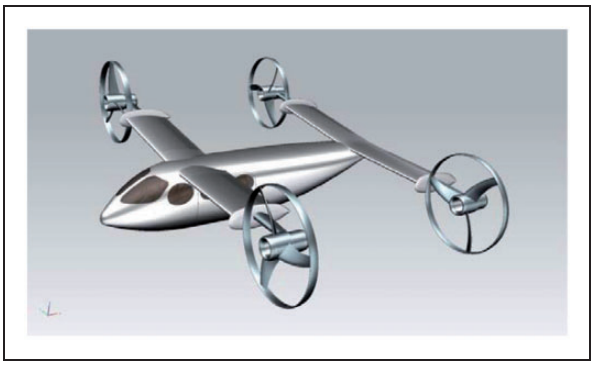

Figure 8. High-speed configuration.

The engines mounted on the rear wing may be used to support lift force and the longitudinal stability or may by turned off. Such case of LS configuration is being presented in Figure 7.

The second flight configuration is the high-speed configuration—HS, which corresponds to horizontal flight presented in Figure 8. All motors are working and all propeller axes are parallel to the longitudinal direction. The total power may be used for the flight. The best performances will be achieved for this configuration.

Other transitive configurations are not presented, although they are going to be considered in further analyses.

Aerodynamic calculations

The unconventional configuration, presented above, can be very promising but requires deep analyses of aerodynamics and flying qualities. Thus the aerodynamic analysis was performed for two important goals. The first one is to obtain the basic aerodynamic characteristics, the second to calculate stability and control derivatives. The aerodynamic analysis was made for two configurations—LS and HS. Moreover, the aircraft's performance (for both speed configurations) has been computed.

As mentioned before, only the complete HS configuration model has been taken into account for the stability analysis. Stability analysis of LS configuration requires not only stability derivatives, but also accurate rotor characteristics, which are not the topic of this paper.

Computational method

The aerodynamic analysis of presented tandem wing configuration was performed using MGAERO Software.[10] The numerical code of software bases on Euler model of flow.[11] A multigrid algorithm[12] is usually used to reduce the computational time. In this case, the multigrid scheme improves convergence of the algorithm. The best way to solve this hyperbolic system of equations is V-cycle scheme of the multigrid method.

Two different types of meshes are necessary for aerodynamic analyses. The first type is the set of mesh, blocks which are used to solve the Euler equations. The second type is surface mesh needed to compute pressure distribution on the aircraft's surfaces. Figure 9 presents the six levels of mesh blocks prepared for model (on the left) and the computational surface mesh which consist of 35,800 panels for the full model (asymmetrical case). The convergence criteria bases on residual and lift force coefficient changes in following iterations. The first criterion is a change in log of the solution residual at each grid level. The second criterion bases on difference between maximum and minimum values of lift force coefficient obtained in the last 10 iterations, performed with the finest grid.

Computational models

Two basic models have been prepared for aerodynamic computation of LS and HS. Both of them

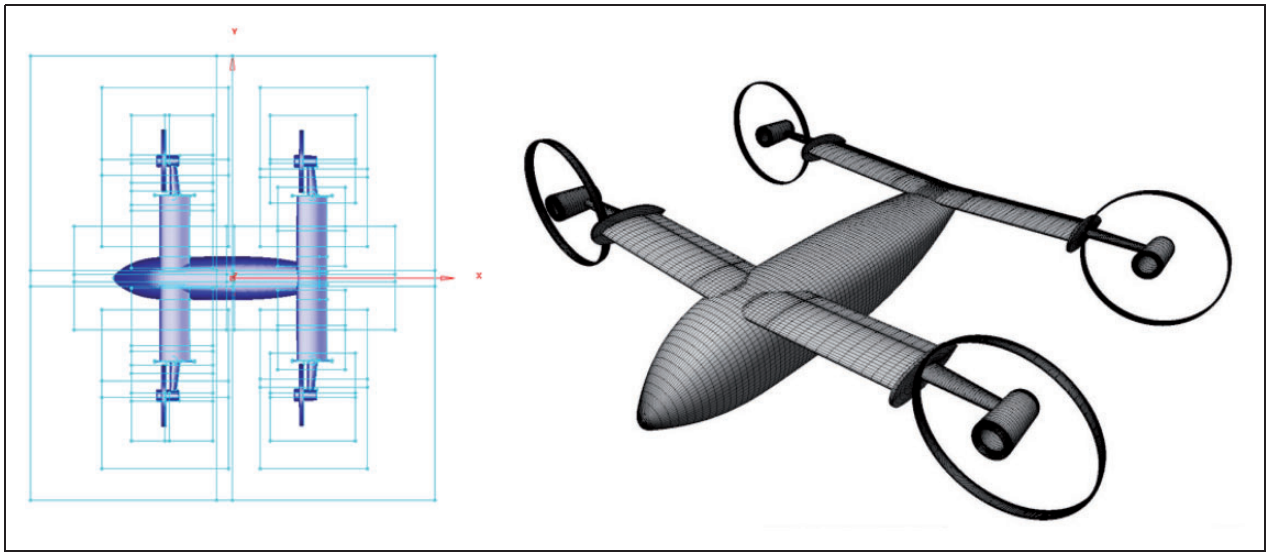

Figure 9. Multigrid blocks (on the left) and computation surface mesh – high-speed aircraft configuration (on the right).

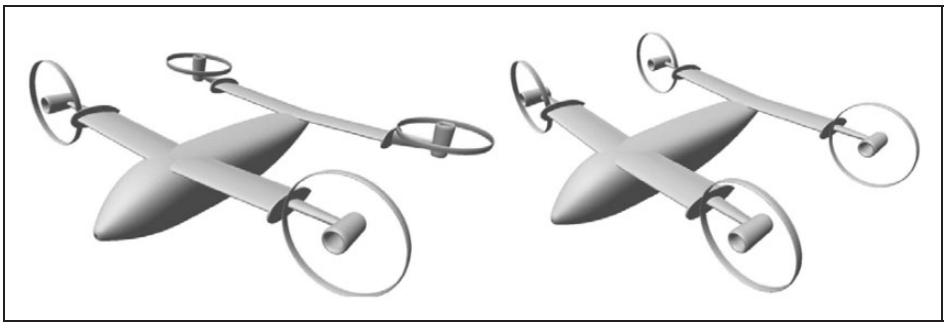

Figure 10. Models used in aerodynamic analysis (LS – left, HS – right).

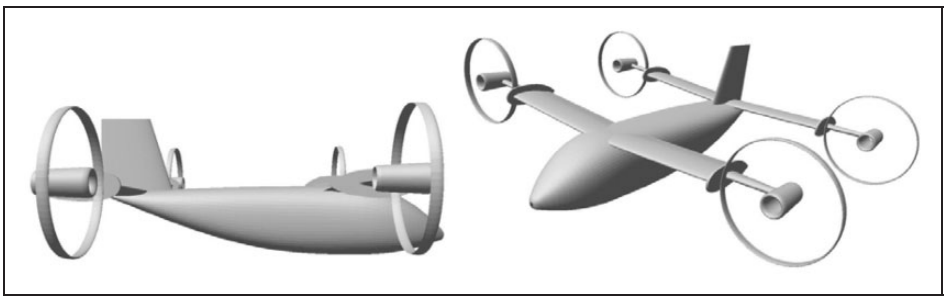

Figure 11. High-speed configuration – model with vertical stabilizer.

consist of the fuselage body and two pairs of wings - forward and rear. Motors with propellers shrouds are modeled by two concentric rings. Figure 10 presents both basic models.

One of the mentioned goals was to calculate the stability and control derivatives. The analysis have been performed, but results of calculations including stability analysis presented below, revealed unsatisfactory values of some stability derivatives, especially in case of lateral characteristics, e.g. C_{nv}. Therefore, it was decided that some modifications to the basic model should be made to satisfy stability requirements. The simplest method was the addition the vertical stabilizer was chosen. The results of previous computations of aircraft without it have been used to assume the required geometry of stabilizer. The area of vertical stabilizer is equal to $S_V = 2$ m^2. Figure 11 presents the modified configuration of the aircraft. Described modifications are connected only with HS and did not change the longitudinal characteristics obtained earlier for HS configuration.

Calculations

Aerodynamic calculation was made for a single Mach number equal to 0.2. Both symmetrical and asymmetrical cases of flow were considered. Moreover, especially for derivatives purpose, the cases of quasi-steady rotations with respect to all axes (yaw, pitch, and roll) were computed. All obtained results are referred to dimensions presented in Table 1.

The aerodynamic analysis was made for LS and HS configurations. The stability derivatives were calculated for HS configuration without and with vertical stabilizer for the same flow conditions. Next, obtained stability derivatives were compared for both models.

Results

The first result of computation of all described models is the C_p distribution on the aircraft's surface. Figure 12 presents aircraft's load for symmetrical cases for LS and HS configuration. The most interesting results were obtained for unsymmetrical cases. As it was mentioned before, two models were taken into account: without and with the vertical stabilizer. The pressure distribution in case of the unsymmetrical velocity distribution for both models is presented in Figures 13 to 15.

Table 1. Reference values.

Reference	Value
Gross wing area (m^2)	10.76
Wing span (m)	5.40
Mean aerodynamic chord (m)	2.00
$X_{25\%MAC}$ (m)	4.00
$Z_{25\%MAC}$ (m)	0.05

Aerodynamic characteristics. The results of computations of the basic aerodynamic characteristics—lift coefficient versus angle of attack and drag polar are presented in Figure 16.

The main differences in aerodynamic characteristics between two presented models come from the configuration of the motors. For both cases the lift force has not changed. The rear pair of motors for the LS configuration significantly increases the drag coefficient and pitching moment. The drag in the LS case is higher than in the HS case. The main reason of this effect is the change of incidence of rear motors axes.

Figure 17 presents the pitching moment versus angle of attack. The reference point is located in 25% of the MAC of the equivalent wing, which is approximately in the middle between both wings. Thus, the pitching moment derivative with respect to angle of attack is positive in a large range of the angles of attack. The CG is located in front of this equivalent wing to satisfy the sufficient static margin.

The analysis of the equilibrium state shows that the deflection angle of elevator necessary to perform trim

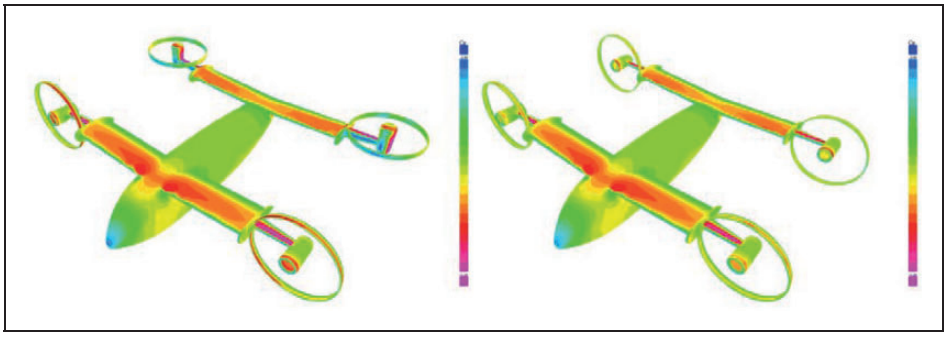

Figure 12. C_p distribution – the LS configuration (left) and the HS configuration (right) for the angle of attack $\alpha = 0^\circ$.

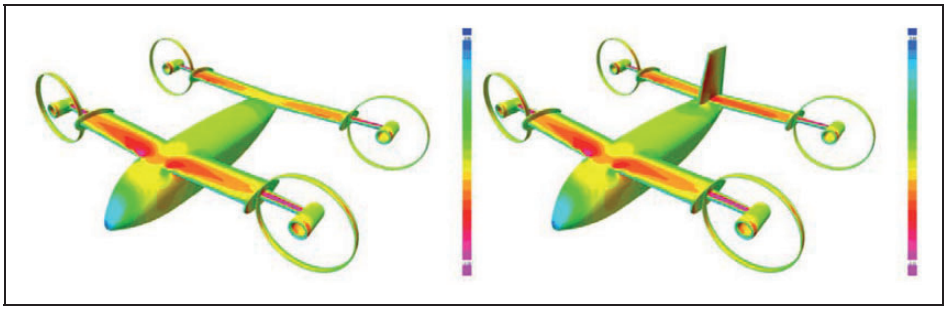

Figure 13. *Cp* distribution for the sideslip angle $\beta = 3^\circ$ aircraft without (left) and with vertical stabilizer (right) (high-speed configuration).

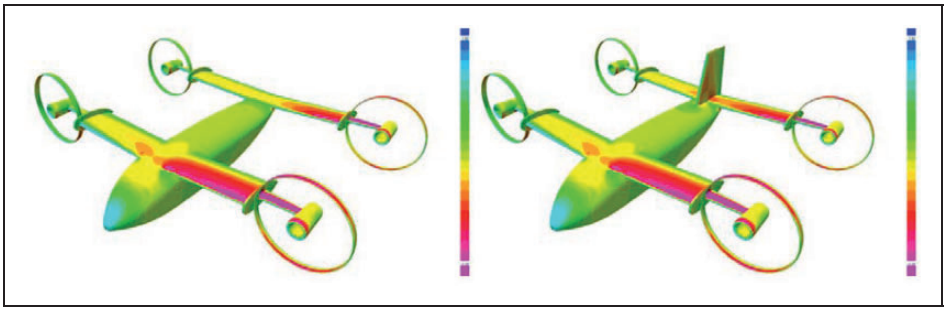

Figure 14. *Cp* distribution for the roll rate $p = 0.2$ rad/s – aircraft without (left) and with vertical stabilizer (right) (high-speed configuration).

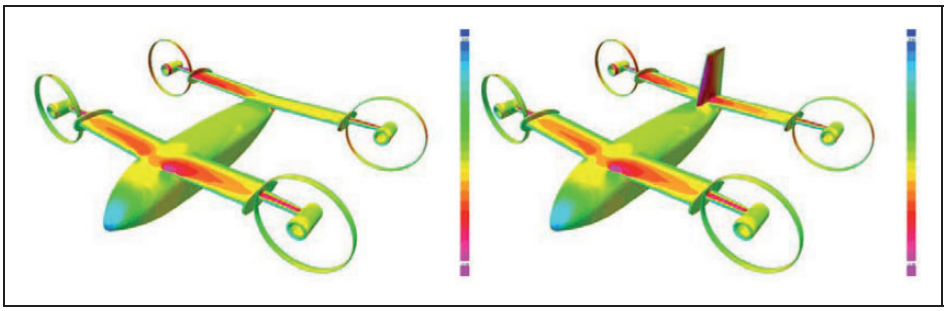

Figure 15. *Cp* distribution for yaw rate $r = 0.2$ rad/s – aircraft without (left) and with vertical stabilizer (right) (high-speed configuration).

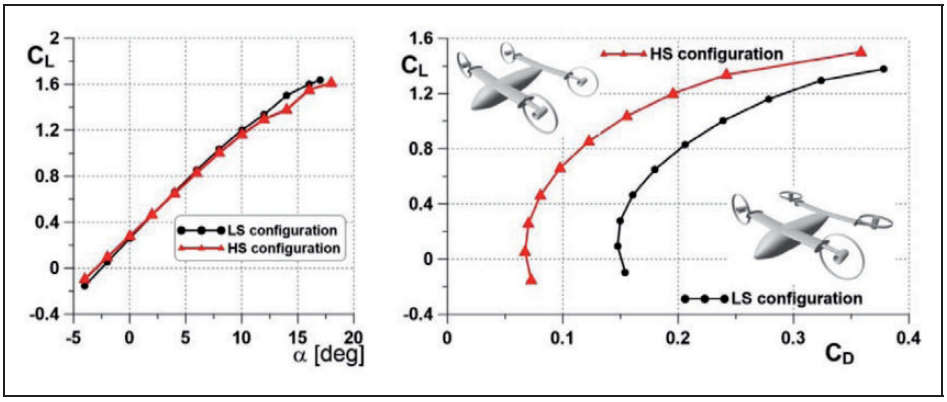

Figure 16. Basic aerodynamic characteristics for LS and HS configurations.
LS: low speed; HS: high speed.

is not large for wide range of angle of attack. Therefore, the efficiency of control surfaces satisfies the control requirements (Figure 18).

Stability derivatives. To determine the stability derivatives a number of cases had to be computed. Symmetrical cases were considered to obtain the longitudinal derivatives and unsymmetrical cases to compute lateral derivatives. It should be noted, that lateral cases are more time consuming due to their asymmetry. Minimum three cases should be computed for each stability derivative. Tables 2 and 3 present the selected stability derivatives computed for both models. Longitudinal cases were computed only for the basic model (without vertical tail) because the influence of vertical stabilizer on longitudinal aerodynamic characteristics can be neglected.

Control derivatives. Stability analysis requires finding the equilibrium state first. Classic longitudinal trim problem is to find the following variables: angle of attack, required thrust, and elevator deflection. In the presented aircraft, the elevator role is fulfilled by the rear wing elevons (Figure 19). Therefore, a few additional computational cases with different deflection of flap have been analyzed. The results are

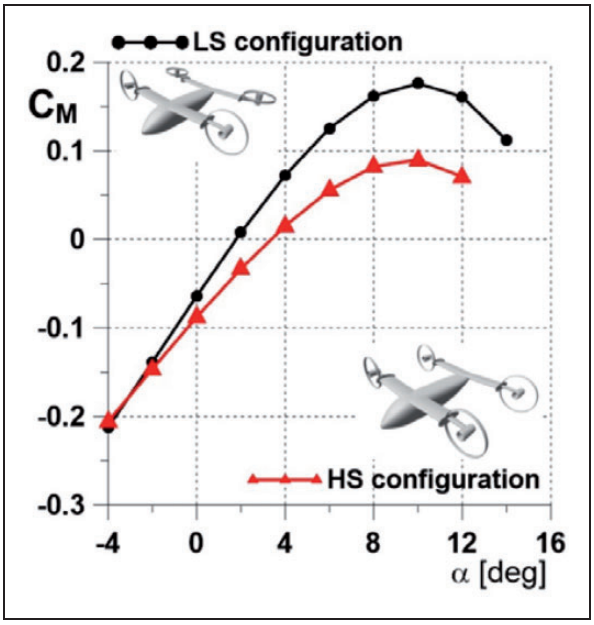

Figure 17. Pitching moment vs angle of attack, for the LS and the HS configuration.
LS: low speed; HS: high speed.

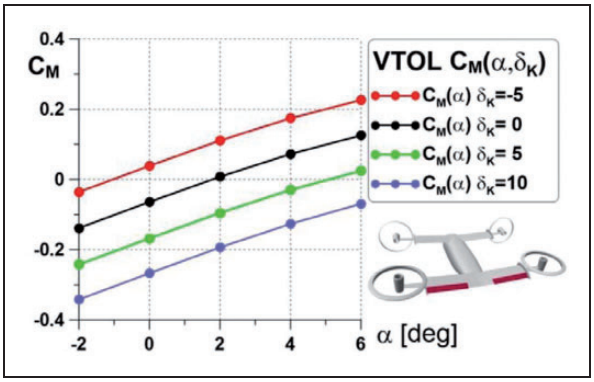

Figure 18. Equilibrium state for low-speed configuration.
VTOL: vertical take-off and landing.

control derivatives—lift force and pitching moment derivatives with respect to flap deflection which allow the solution to the trim problem.

Performance

The basic performance characteristics including flight envelope, range, and endurance were calculated for both configurations in order to test if they meet the project assumptions and if they are satisfying. Figures 20 and 21 present results of performance analysis obtained for maximum take-off weight and with assumption, and that motors' power does not change with altitude. Such assumption can be used due to the electric motor altitude characteristics—no loss of power versus altitude caused by pressure decrease.

The computed performance characteristics—high maximum airspeed, ceiling, and rate of climb are accordant to assumed values. The endurance and range (Figure 22) were calculated only for the HS configuration.

Table 2. Longitudinal stability derivatives.

Stability derivatives	Value
Cdw	0.186
CLw	5.855
CLq	−0.734
Cmw	1.650
Cmq	−2.725

Table 3. Lateral stability derivatives.

Stability derivatives	Basic model	Aircraft with vertical stabilizer
Cyv	−0.853	−1.287
Cyp	0.072	0.097
Cyr	−0.052	−0.100
Clv	−0.636	−0.785
Clp	−0.254	−0.262
Clr	0.017	0.018
Cnv	−0.468	−0.281
Cnp	−0.021	−0.017
Cnr	−0.061	−0.092

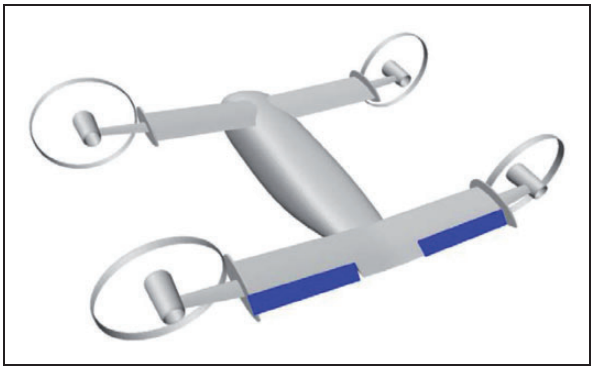

Figure 19. Model of the HS configuration with rear wing control surfaces.

Stability analysis

Stability analysis of presented tandem-wing aircraft was performed using SDSA (Simulation and Dynamic Stability Analysis) software package.[13] First of all, the package was developed to analyze the stability of an aircraft. It can compute stability characteristics of both uncontrolled (fixed controls) and controlled (pilot in the loop) aircraft. It also has embedded 6 DoF desktop flight simulator, LQR-based FCS, performance module, etc. The SDSA[14] was designed to use the

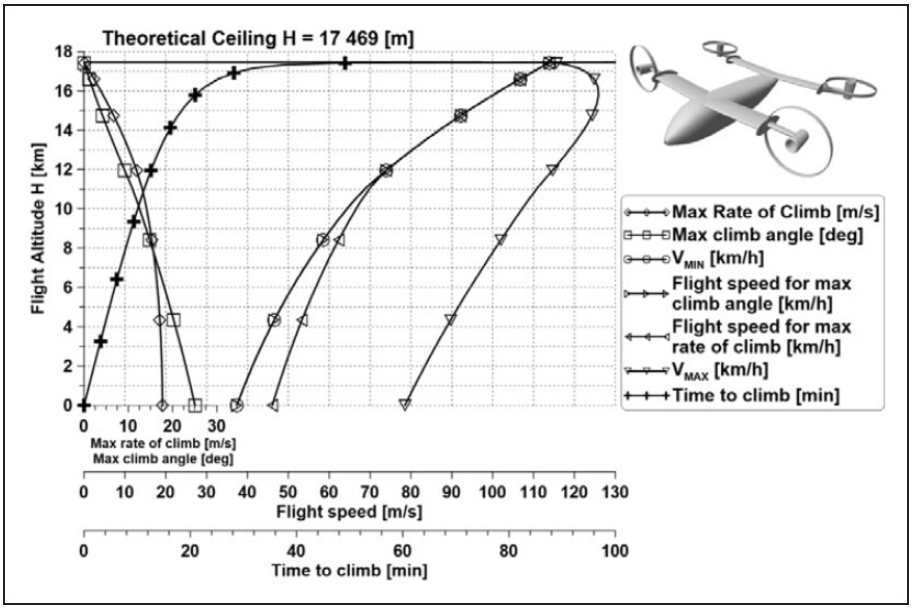

Figure 20. Flight envelope for the LS ($m = 1600$ kg).

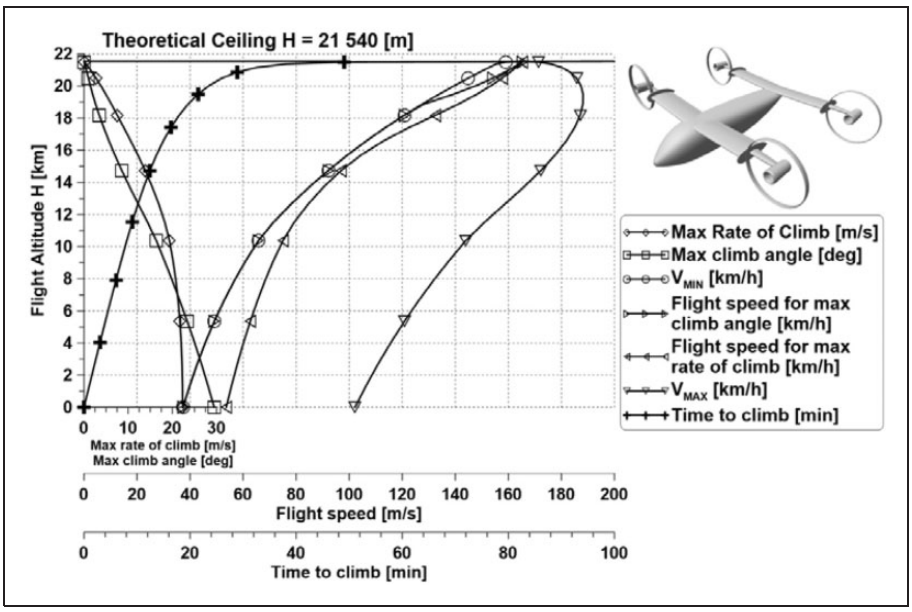

Figure 21. Flight envelope for the HS ($m = 1600$ kg).

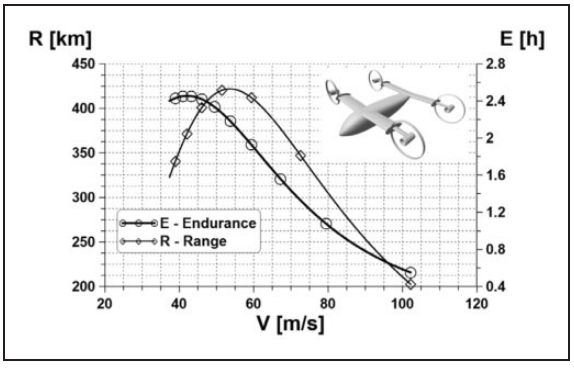

Figure 22. Range and endurance for the HS configuration ($H = 0$ m, $V =$ const., $\eta_{prop} = 0.8$, $m = 1600$ kg).

same nonlinear model[15–20] of the aircraft motion for each functionality (stability, simulation, performance). For eigenvalues analysis, the nonlinear model was linearized numerically by computing the Jacobian matrix of the state derivatives in the equilibrium (trim) point. It allowed the construction of the stability analyzer using the same set of equations as in the flight simulation. The flight simulation module, based on mathematical model with six degrees of freedom, can be used to do test flights in order to record flight parameters in real time. Next they can be used for identification of typical modes of motions and their parameters (period, damping coefficient, phase shift). The stability analysis results are presented in the figures of merits based on JAR/FAR, ICAO, MIL[21] regulations.

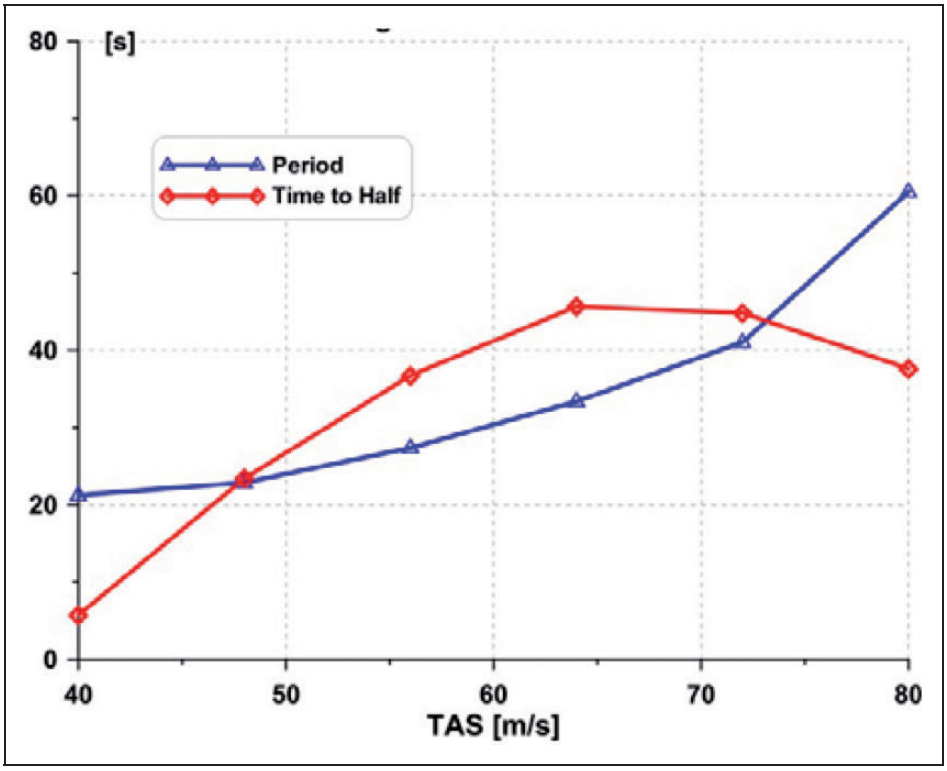

Figure 23. Phugoid characteristics: Period and time to half damping.

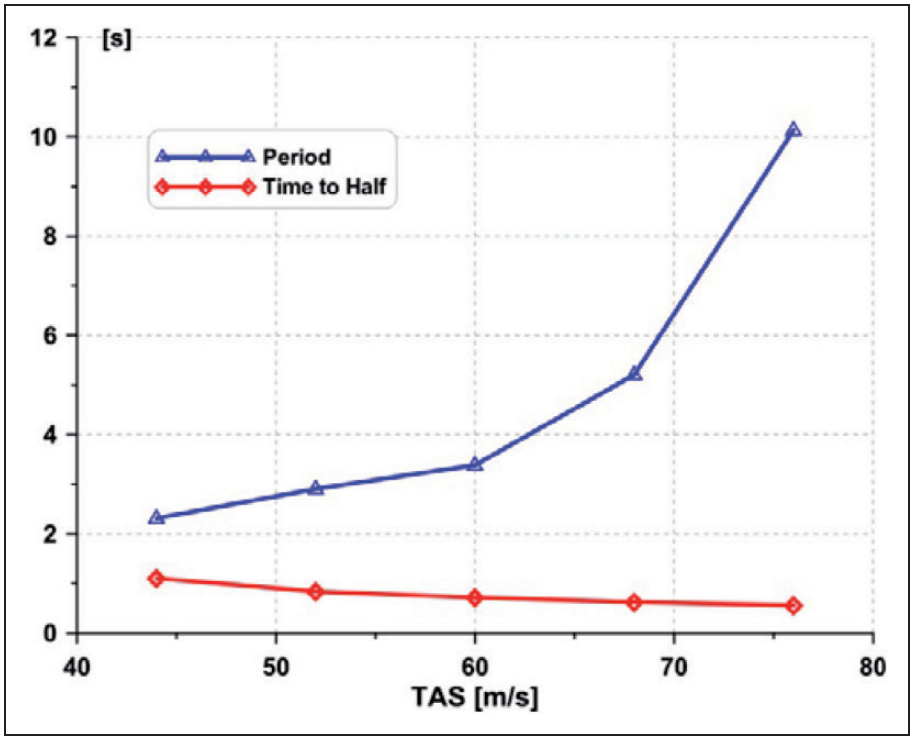

Figure 24. Short period characteristics: Period and time to half damping.

Configuration without vertical tail (original design)

In the first stage, the stability characteristics were calculated for original configuration, without vertical tail. The vertical stabilizer does not influence the longitudinal modes, so only lateral modes were analyzed and compared for both configurations.

Longitudinal modes. Both longitudinal modes proved to be stable. Figure 23 presents the period and time

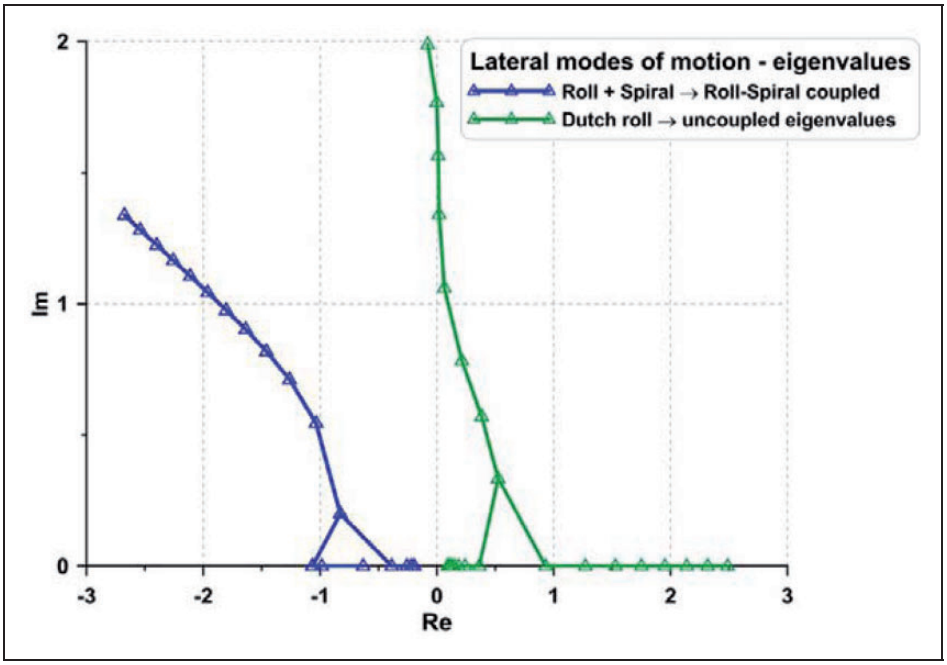

Figure 25. Lateral modes – eigenvalues.

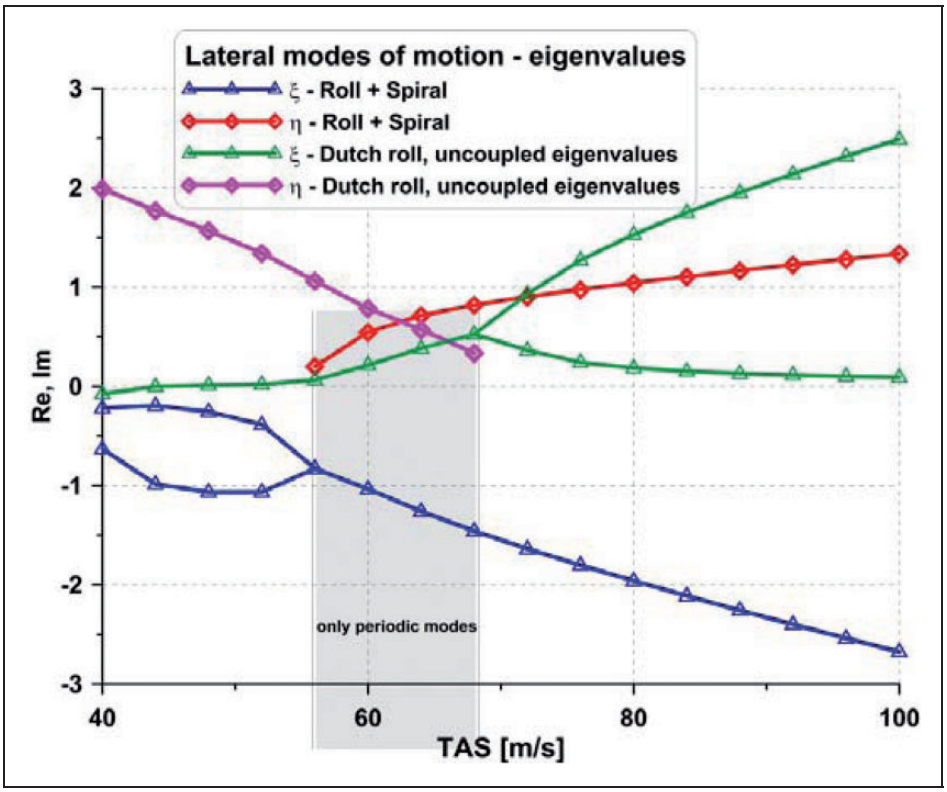

Figure 26. Lateral modes – real and imaginary parts of eigenvalues.

to half damping for phugoid mode. The results show that although the mode is stable, the time to half damping is long and could be longer than period, which could lower the pilot rating. Figure 24 presents the same variables for short period mode. The mode is stable; however, time to half damping is comparable with period for low airspeed, which could turn out to be unacceptable.

Lateral modes. The original design does not have a vertical stabilizer and lateral derivatives with respect to sideslip angle show that configuration could

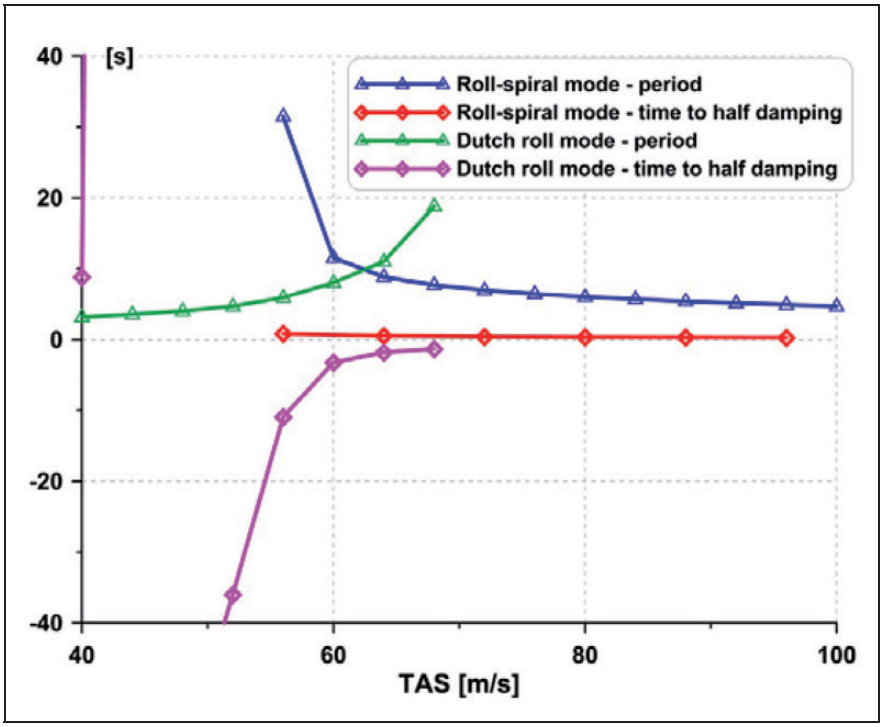

Figure 27. Lateral periodical modes – period and time to half damping.

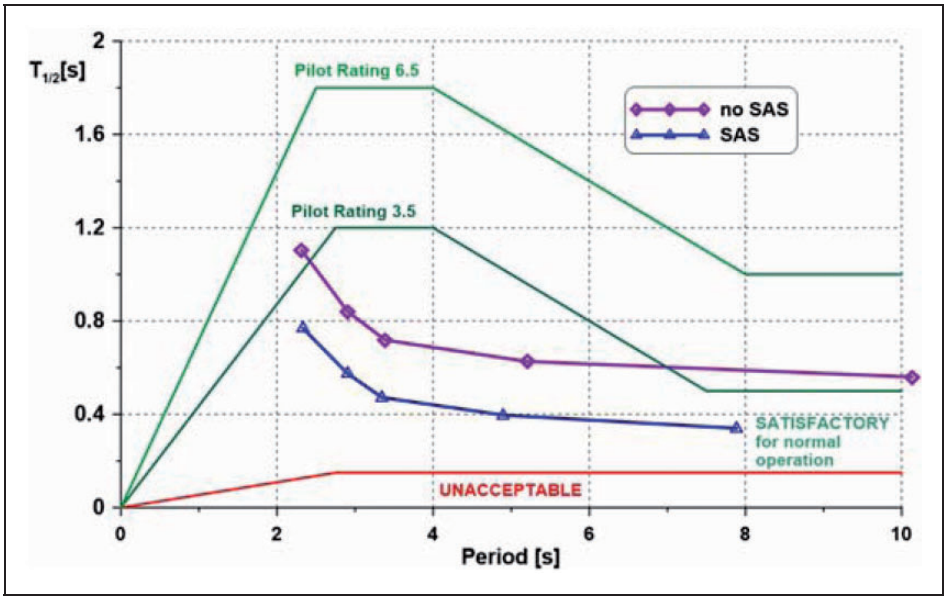

Figure 28. Short period characteristics: ICAO-based figure of merit – time to half damping versus period – without and with SAS system.
SAS: stability augmentation system.

be unstable. Especially the derivative of yawing moment with respect to sideslip angle is strongly negative, which is not good from stability point of view. Two tilt-rotors mounted on the wing tips could improve lateral characteristics; however, flight should be stable also in case of motor cut off (e.g. motor failure).

Figure 25 presents lateral eigenvalues, imaginary part versus real one. The results are interesting and not typical. In a certain range of airspeeds (Figure 26), there are two periodic modes—Dutch roll and so called roll-spiral, both coupled. In all airspeeds outside of this range, at least one of the modes is uncoupled.

Unfortunately the lateral characteristics are not good. Dutch roll is not damped well and to some extent even unstable (Figure 27). The roll-spiral mode is also very poorly damped. These results

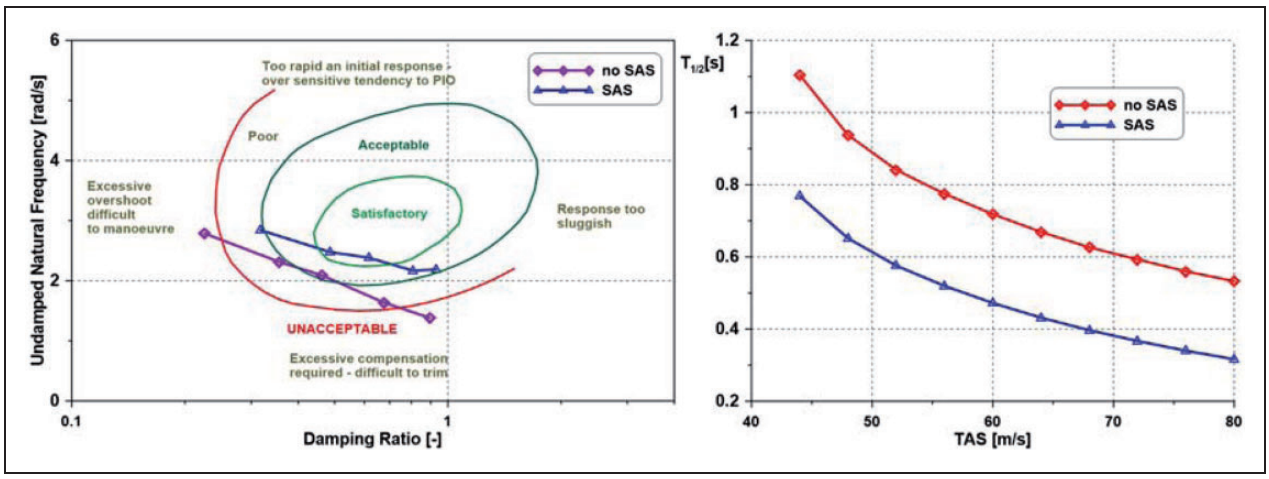

Figure 29. Short period characteristics: ESDU-based figure of merit and time to half damping – without and with SAS system. SAS: stability augmentation system.

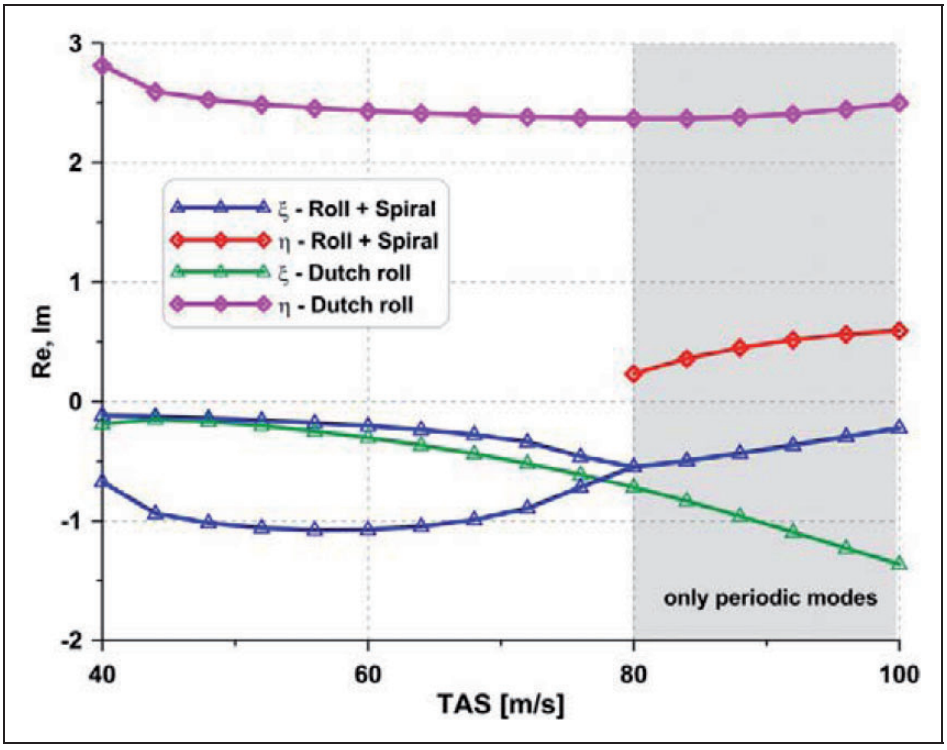

Figure 30. Lateral modes – real and imaginary parts of eigenvalues.

show that some improvements have to be made to satisfy stability criteria for lateral modes of motion.

Improvements

The results of stability analysis of the original design showed that configuration has to be improved. The longitudinal modes of motion should be damped better, while lateral modes, especially Dutch roll must be stabilized. The longitudinal characteristics were improved by control system—simple stability augmentation system (SAS). The lateral modes were improved by additional a vertical stabilizer.

Improvement of flying qualities by control system. The longitudinal modes of motion, especially short period mode, needed to be improved. It was assumed, that SAS will be applied to increase damping. First tests carried out in the SDSA have confirmed that this approach should be effective. Figures 28 and 29 present the results of stability analysis performed for both configurations: with and without the SAS system. Presented figures of merit show that the pilot rating for aircraft with SAS is significantly better and quite satisfying.

Improvement by geometry modification. The original design was a strongly unstable configuration, which

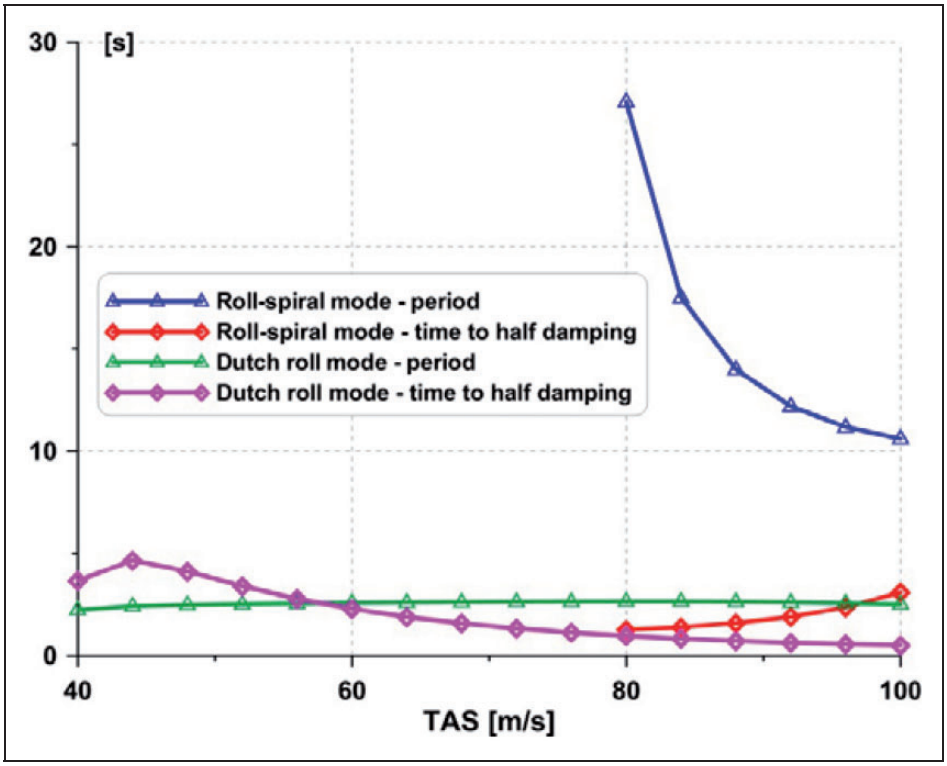

Figure 31. Lateral periodical modes – period and time to half damping.

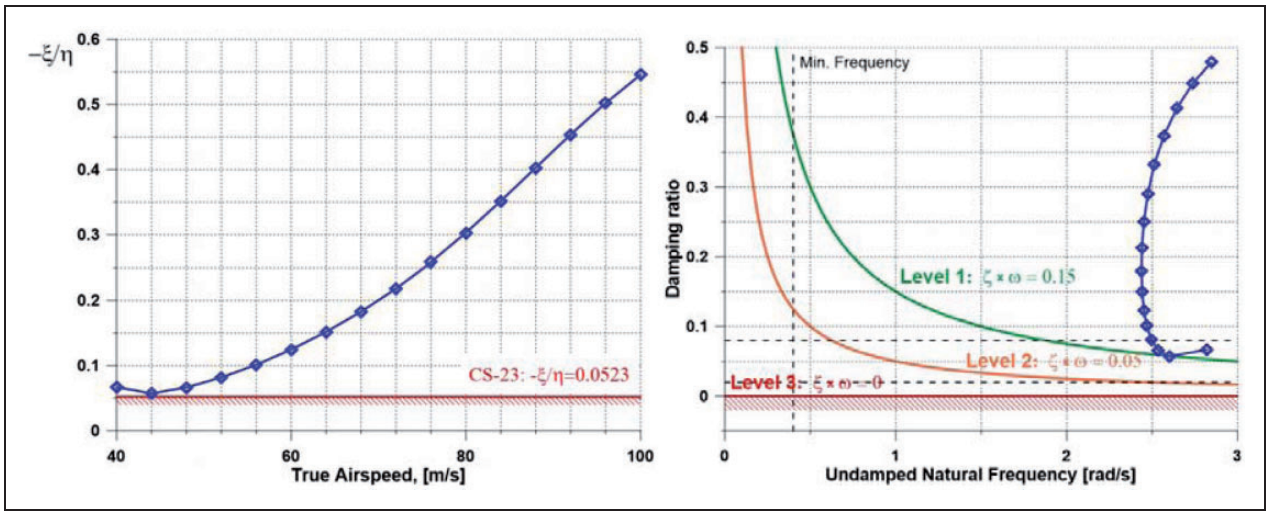

Figure 32. Dutch roll mode – figures of merit based on: CS-23 (left) and MIL-F-8785C (right) criteria.

was described before. The addition of the vertical stabilizer improved lateral characteristics to a satisfying level. Figure 30 presents eigenvalues of lateral modes of motion (real and imaginary part). It shows that all modes are stable; however, still in a certain range only periodic modes are present. Figure 31 presents period and time to half damping for both periodic modes of motion.

Figure 32 presents Dutch roll characteristics against background of figures of merit based on CS-23 regulation and MIL-F-8785C criteria. MIL criteria were also used to rate roll-spiral mode (Figure 33). The rating of both lateral modes (especially Dutch-roll) is high (1st level); however, spiral-roll rating for higher airspeed is a little worse.

Figure 34 presents desktop simulator embedded in SDSA during simulation of lateral modes of presented aircraft. Figure 35 presents results of the simulation. The initial equilibrium state was disturbed by initial sideslip angle. Presented graph shows strongly damped Dutch roll and after that, visible long period spiral-roll mode.

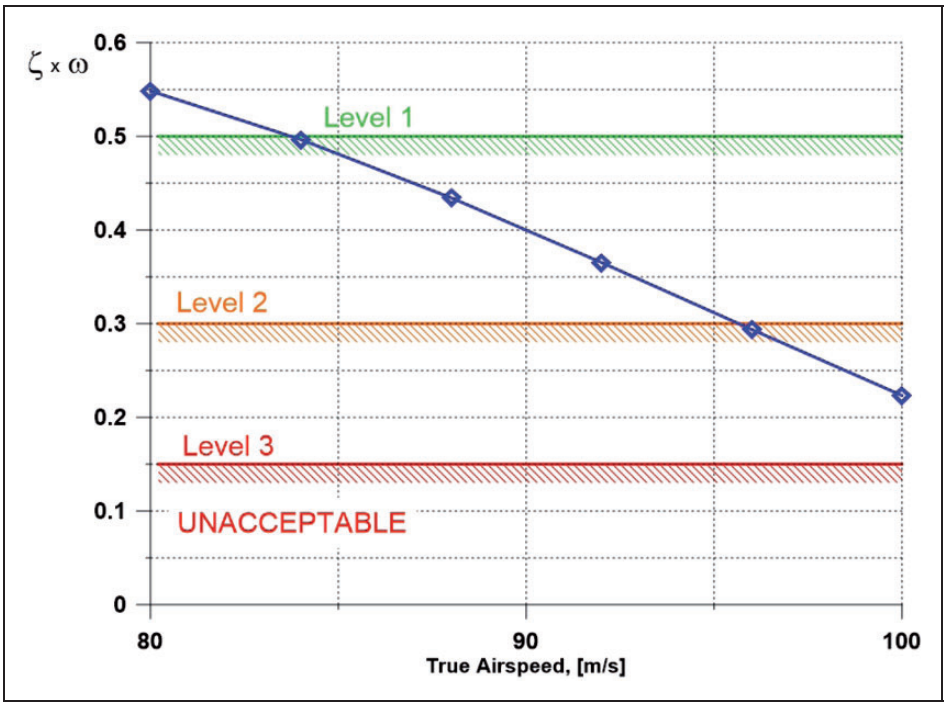

Figure 33. Roll-spiral mode – figure of merit based on MIL-F-8785C criteria.

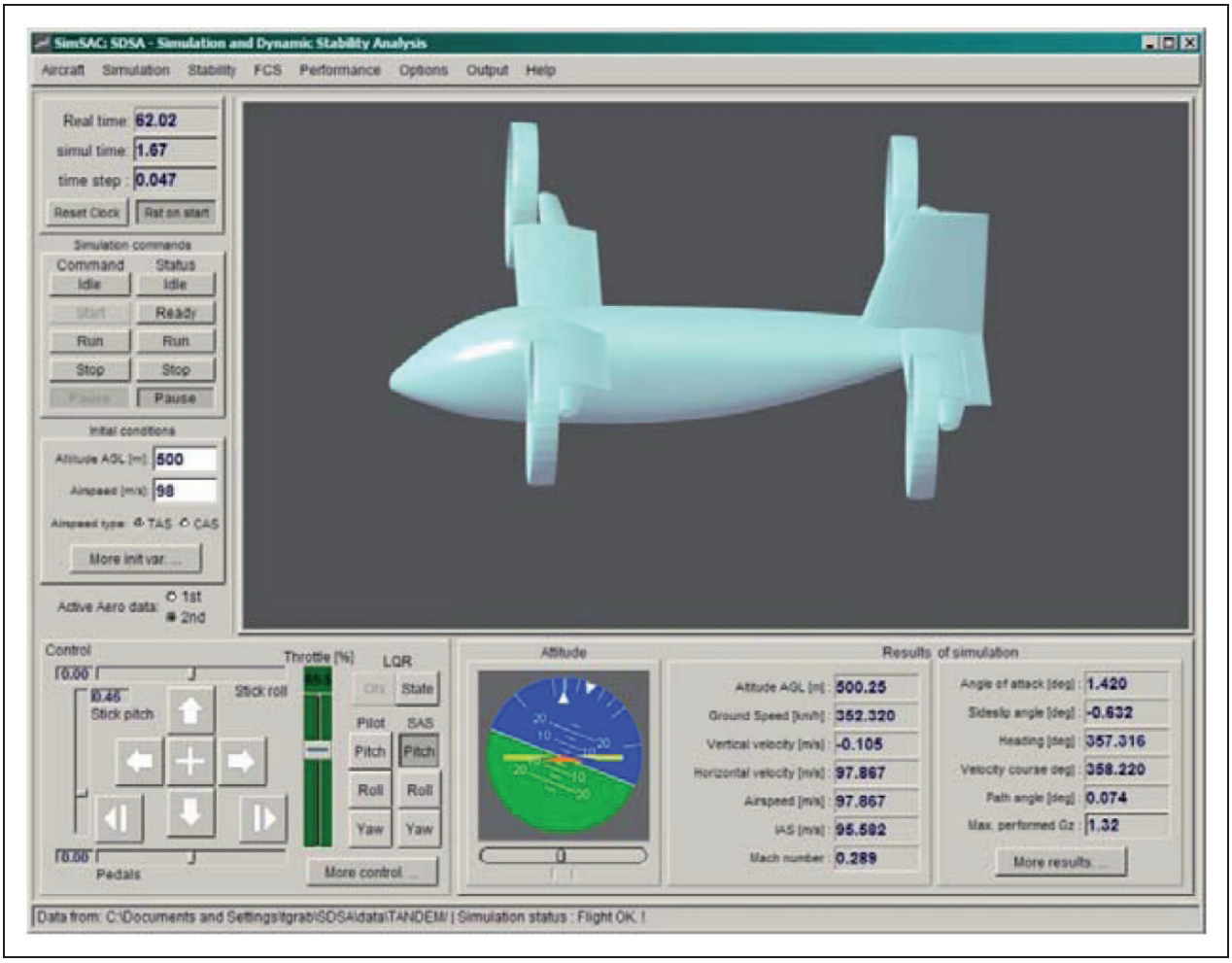

Figure 34. Flight simulation of analyzed aircraft.

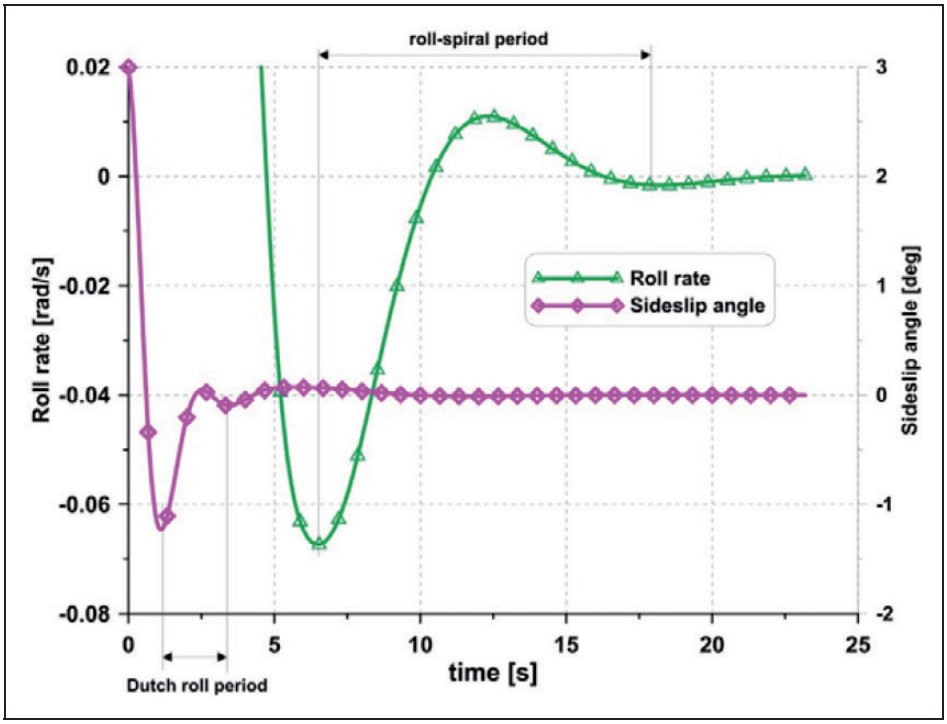

Figure 35. Flight simulation results of lateral oscillations.

Concluding remarks

The tandem wing configuration seems to be very promising despite the fact that such unconventional configuration can cause some problems with flying qualities. The VTOL and STOL functionalities connected with relatively high speed can be a good choice for PPlane system and any other personal airplane. The proposed aircraft satisfies short door to door time by reducing the take-off and landing distance and in consequence allows easy access to the airfield. It can be also used as a multipurpose air vehicle, including special applications such as air ambulance or police patrol. The high cruise speed supplements good performance characteristics.

The stability analysis shows that despite unconventional configuration and in consequence unconventional behavior (i.e. two lateral periodic modes), the proposed vehicle can be designed as stable. Moreover, sufficient flight control system should be a good solution to improve flying qualities and to obtain well rated pilot opinion.

Declaration of Conflicting Interests

The author(s) declared no potential conflicts of interest with respect to the research, authorship, and/or publication of this article.

Funding

The author(s) disclosed receipt of the following financial support for the research, authorship, and/or publication of this article: This study was supported by the European Commission through co-funding of the FP7 project PPLANE.

References

1. PPLANE – the Personal Plane Project. Assessment and validation of pioneering concepts for personal air transport systems. Grant agreement no.: 233805, Annex 1, 30 June 2009.
2. Giulietti F and Gatti M. Report on the definition of operational and technical parameters and requirements for PPlane systems. PPLANE Deliverable D1.1, 2011.
3. Le Tallec C and Joulia A. Baseline PPlane system description. PPLANE Deliverable 6.0, 2012.
4. Le Tallec C and Harel M. A personal plane air transportation system: The PPlane Project. In: *28th congress of the international council of the aeronautical sciences*, Brisbane, Australia, Paper ICAS 2012-10.5.1, 23–28 September 2012.
5. Goetzendorf-Grabowski T. Application of house of quality tool into the analysis of operational concept for the future personal air transportation system. In: *Proceedings of READ 2010 conference*, Warsaw, 2010.
6. Figat M, Goraj Z and Grendysa W. Preliminary concept for energetic model of PPLANE. In: *Presentation on PPLANE meeting*, Madrid, 27–28 September 2010.
7. Buttler T. *British Secret Projects Fighters & Bombers, 1935–1950*. Hinckley: Midland Publications, 2004.
8. http://www.scaled.com/projects/proteus
9. http://www.scaled.com/projects/advanced_technology_tactical_transport_attt
10. MGAERO A Cartesian multigrid Euler code for flow around arbitrary configurations - User's manual version 3.1.4.

11. Anderson JD Jr. *Computational fluid dynamics – The basis with applications*. New York: McGraw-Hill, Inc., 1995.
12. Mavriplis DJ. Three-dimensional unstructured multigrid for the Euler equations. *J Aircraft* 1992; 30.
13. Goetzendorf-Grabowski T. SDSA – Simulation and dynamic stability analysis – software package. Warsaw University of Technology, http://www.meil.pw.edu.pl/add/ADD/Teaching/Software/SDSA
14. Goetzendorf-Grabowski T, Mieszalski D and Marcinkiewicz E. Stability analysis using SDSA tool. *Prog Aerosp Sci* 2011; 47: 636–646.
15. Goetzendorf-Grabowski T. Modelling of the aircraft motion - theory and application. In: *Optimalsteuerungsprobleme von Hyperschall-Flugzeugsystemen*, Workshop des Sonderforshungsbereichs 255, Greifswald-München, 1997, pp.21–34.
16. Etkin B. *Dynamics of flight - Stability and control*. New York: John Wiley & Sons, Inc., 1982.
17. Cook BH. *Flight dynamics principles*. Cranfield: Butterworth Heinemann, 1997.
18. Stevens BL and Lewis FL. *Aircraft control and simulation*. New York: John Wiley & Sons, Inc., 1992.
19. Nelson RC. *Flight stability and automatic control*. 2nd ed. New York: McGraw-Hill, 1998.
20. Goraj Z. Flight dynamics models used in different national and international projects. *Aircraft Eng Aerosp Technol* 2014; 86: 166–178.
21. MIL-F-8785C - Military specification flying qualities of piloted airplanes, 5 November 1980.